Bol. Soc. Paran. Mat.
©SPM – E-ISSN-2175-1188
SPM: www.spm.uem.br/bspm

(3s.) **v. 2026 (44) 3** : 1–14.
ISSN-0037-8712
doi:10.5269/bspm.80140

Variational and Numerical Study for Eigenvalues Double-Phase Elliptic Problems with Robin Boundary Conditions

Abdelaziz El Baraymi, Youness El Yazidi and Bouchaib Ferrahi

ABSTRACT: In this paper, we study the numerical approximation of the first eigenvalue in double-phase equation subject to Robin boundary conditions. When the parameters of this problem satisfy certain assumptions, particularly regarding the right-hand side function, we establish the existence of the first eigenvalue with its corresponding eigenfunction. The Physics-Informed Neural Networks approach is considered to approximate this solution. At the end, we conduct several numerical test for different exponents and analytical solution.

Key Words: Double-phase problem, Robin boundary conditions, Physics-Informed Neural Networks.

Contents

1. Introduction

In the present work, we investigate solutions to the corresponding nonlinear eigenvalue problem:

$$\begin{cases} -\operatorname{div}\big(|\nabla u|^{p-2}\nabla u+\mu(x)|\nabla u|^{q-2}\nabla u\big)=\lambda f(x,u), & \text{in } \Omega,\\ \big(|\nabla u|^{p-2}\nabla u+\mu(x)|\nabla u|^{q-2}\nabla u\big).\vec{n}+\beta(x)|u|^{r-2}u=g, & \text{on } \partial\Omega, \end{cases} \qquad (P_\lambda)$$

where Ω is a bounded smooth domain in $\mathbb{R}^{\mathbb{N}}$ with Lipschitz boundary $\partial\Omega$, $\vec{n}$ denotes the unit outward normal to $\partial\Omega$, the exponents p , q and r satisfy $1<p<q<N$, and $1<r\le p_*=\dfrac{p(N-1)}{N-p}$, while β lies in $L^\infty(\partial\Omega)$ and satisfies $\beta^-:=\inf_{x\in\partial\Omega}\beta(x)>0$. The function f satisfies certain assumptions on $\Omega\times\mathbb{R}$ that will be specified later; The parameter λ is a positive real number, and g denotes the boundary data.

Recently, double-phase problems gained a lot of attention, for example in [4] a first numerical approximation of double phase problem was performed using the finite element method. The study of eigenvalue problems associated with the double-phase problem has also received growing focus, due to their importance in the mathematical modeling of various physical phenomena.

For example, the problem (P_λ) can be used to model the diffusion of a substance or the propagation of heat in a heterogeneous and nonlinear material. The coefficient $\mu(x)$ represents a spatial variation of the conductivity, which increases toward the domain boundary. The function $f(x,u)$ represents a local nonlinear reaction associated with an external source. On the boundary $\partial\Omega$, the nonlinear Robin condition expresses the nonlinear exchange between the medium and its environment, modeling for example an energy loss or a heat flux proportional to a power of u. The parameter $\lambda>0$ controls the intensity

2020 *Mathematics Subject Classification:* 35K15, 35R30, 65D12, 90C53.
Submitted November 15, 2025. Published January 22, 2026

of the internal reaction. This model thus illustrates a nonlinear diffusion–reaction system in a heterogeneous medium, allowing the study of complex physical phenomena such as anomalous conduction, non-Newtonian flows, or nonlinear heat transfer processes.

Theoretically, the majority of existing studies in the literature concern the study of problem (P_λ) under Dirichlet boundary conditions or when a convection term is added. For example, Gasinski et al in [5] considered the following equation:

$$\begin{cases} -\operatorname{div}\big(|\nabla u|^{p-2}\nabla u + \mu(x)\,|\nabla u|^{q-2}\nabla u\big) = f(x,u,\nabla u), & \text{in } \Omega, \\ u = 0, & \text{on } \partial\Omega. \end{cases} \tag{1.1}$$

Using the theory of pseudomonotone operators and under certain linear conditions on the gradient, the authors proved the existence and uniqueness of a solution to problem (1.1). The case of Robin boundary conditions has also been investigated by several authors using various methods. For instance, Papageorgiou et al. [10,8,9] demonstrated that problem (P_λ) admits a unique solution in certain specific cases, one of which is defined as follows:

$$\begin{cases} -\operatorname{div}\big(a(z)\,|\nabla u|^{p-2}\nabla u\big) - \Delta_q u + \xi(z)\,|u|^{p-2}u = \lambda\, f(z,u(z)), & \text{in } \Omega, \\ \dfrac{\partial u}{\partial n_\vartheta} + \beta(z)\,|u|^{p-2}u = 0, \quad 1<q<p<+\infty, & \text{on } \partial\Omega. \end{cases} \tag{1.2}$$

On the other hand, from a numerical point of view, we have not found many works that explicitly address the numerical approximation of double-phase problems.
Consequently, the numerical investigation of this type of problem is highly relevant and represents a genuine contribution to scientific research.

Motivated by the theoretical results discussed above, this work focuses on the investigation of the first eigenvalue of problem (P_λ), characterised by the following expression:

$$\begin{aligned} \lambda_1 &= \min_{\substack{u\in W^{1,\mathcal{H}}(\Omega)\\ u\neq 0}} J(u) \\ &= \min_{\substack{u\in W^{1,\mathcal{H}}(\Omega)\\ u\neq 0}} \left[\int_\Omega \left(\frac{1}{p}|\nabla u|^p + \mu(x)\frac{1}{q}|\nabla u|^q\right)dx + \int_{\partial\Omega}\frac{1}{r}\beta|u|^r\,ds - \lambda\int_\Omega F(x,u)\,dx - \int_{\partial\Omega} g\,u\,ds\right]. \end{aligned}$$

where

$$F(x,t) = \int_0^t f(x,s)ds.$$

Subsequently, assuming appropriate constraints on the problem parameters, we demonstrate the well-posedness of the eigenvalue problem and develop a reliable numerical scheme using Physics-Informed Neural Networks (PINNs) for the simultaneous estimation of the eigenvalue and its corresponding eigenfunction.

The paper is organized as follows. Section 2 presents the basic notions and properties of the relevant functional spaces, along with the principal existence results related to problem (P_λ). Section 3 focuses on the spectral analysis of the problem, while section 4 outlines the numerical framework employed to address the nonlinear eigenvalue problem. Lastly, section 5 reports and interprets the obtained numerical results.

2. Preliminaries

In this section, we present some essential notions from functional analysis required for the later analysis. We begin with some key properties of the Lebesgue and Sobolev spaces $L^p(\Omega)$ and $W^{1,p}(\Omega)$.

Consider a bounded domain $\Omega \subset \mathbb{R}^N$ $(N \geq 1)$ whose boundary $\partial\Omega$ is Lipschitz continuous, for every $1 \leq p < \infty$ we denotes by $L^p(\Omega)$ the usual Lebesgue spaces defined as

$$L^p(\Omega) = \{u : \Omega \to \mathbb{R}, u \quad \text{measurable and} \quad \int_\Omega |u(x)|^p < +\infty\}$$

equipped with the norm given by:

$$||u||_{0,p} = \left[\int_\Omega |u(x)|^p dx\right]^{\frac{1}{p}}$$

According to the result of [12], $(L^p(\Omega), ||\cdot||_{0,p})$ is reflexive, separable, and defined a uniformly convex Banach space.
And for $1 < p < \infty$, we consider the corresponding Sobolev space $W^{1,p}(\Omega)$ defined as

$$W^{1,p}(\Omega) = \{u \in L^p(\Omega) : |\nabla u| \in L^p(\Omega)\}$$

endowed with the norms $||.||_{1,p}$ given by

$$\|u\|_{1,p} = ||u||_{0,p} + ||\nabla u||_{0,p}$$

and

$$\|u\|_* := \left(\int_\Omega |\nabla u|^p \, dx + \int_{\partial\Omega} \beta |u|^p \, ds\right)^{\frac{1}{p}}$$

It is well known that the norms $\|u\|_{1,p}$ and $\|u\|_*$ are equivalent, and that the space $\left(W^{1,p}(\Omega), \|\cdot\|_{1,p}\right)$ is a separable, reflexive, and uniformly convex Banach space [7].
If $u \in L^p(\Omega)$ and $v \in L^{p'}(\Omega)$ such that $1 < p < \infty$ with $\frac{1}{p} + \frac{1}{p'} = 1$, then we have the following estimate known as Hölder's inequality [12]: $uv \in L^1(\Omega)$ and

$$\left|\int_\Omega uv \, dx\right| \leq \|u\|_{0,p} \, \|v\|_{0,p'}$$

On the other hand, we know that $W^{1,p}(\Omega) \hookrightarrow L^{\hat{p}}(\Omega)$ is compact for $\hat{p} < p^*$ and continuous for $\hat{p} = p^*$, where p^* is the critical exponent of p defined by

$$p^* = \begin{cases} \dfrac{Np}{N-p}, & \text{if } p < N, \\ +\infty, & \text{if } p \geq N. \end{cases} \tag{2.1}$$

We equipped the boundary Lebesgue space $L^p(\partial\Omega)$ with the norm $||.||_{\partial\Omega}$. It is well known that the mapping $W^{1,p}(\Omega) \hookrightarrow L^{\tilde{p}}(\partial\Omega)$ is compact for for $\tilde{p} < p_*$ and continuous for $\tilde{p} = p_*$, where p_* is the critical exponent of p on the boundary given by

$$p_* = \begin{cases} \dfrac{(N-1)p}{N-p}, & \text{if } p < N, \\ +\infty, & \text{if } p \geq N. \end{cases} \tag{2.2}$$

Throughout this paper, we shall assume that

$$1 < p < q < N, \quad 1 < r < p_* \quad \text{and} \quad 0 \leq \mu(.) \in L^1(\Omega). \tag{2.3}$$

Consider the function $\mathcal{H} : \Omega \times [0, 1) \to [0, 1)$ defined by

$$\mathcal{H}(x, t) = t^p + \mu(x)t^q.$$

and the following modular function defined by

$$\rho_{\mathcal{H}}(u) := \int_\Omega \mathcal{H}(x, |u|) \, dx = \int_\Omega \left(|u|^p + \mu(x)|u|^q\right) dx.$$

Next, we define the Musielak–Orlicz space $L^{\mathcal{H}}(\Omega)$ by

$$L^{\mathcal{H}}(\Omega) = \{\, u : \Omega \to \mathbb{R} \text{ measurable such that } \rho_{\mathcal{H}}(u) < +\infty \,\},$$

equipped with the Luxemburg norm

$$\|u\|_{\mathcal{H}} = \inf \left\{ \lambda > 0 : \rho_{\mathcal{H}}\Big(\frac{u}{\lambda}\Big) \leq 1 \right\}.$$

Therefore , we introduce the Musielak-Orlicz Sobolev space $W^{1,\mathcal{H}}(\Omega)$ which is defined by

$$W^{1,\mathcal{H}}(\Omega) = \Big\{ u \in L^{\mathcal{H}}(\Omega) : |\nabla u| \in L^{\mathcal{H}}(\Omega) \Big\},$$

equipped with the norm

$$\|u\|_{1,\mathcal{H}} = \|u\|_{\mathcal{H}} + \|\nabla u\|_{\mathcal{H}},$$

where

$$\|\nabla u\|_{\mathcal{H}} = \|\, |\nabla u| \,\|_{\mathcal{H}}.$$

According to the result of [2] , the spaces $(L^{\mathcal{H}}(\Omega), ||.||_{\mathcal{H}})$, and $(W^{1,\mathcal{H}}(\Omega), ||.||_{1,\mathcal{H}})$ are reflexive, separable, and Banach spaces.
Now, we recall some important results from [1]:

Proposition 1 *Assume that (2.3) holds and let p^* and p_* be the critical exponent defined in (2.1) and (2.2). Then, the following embeddings hold:*

- $L_{\mathcal{H}}(\Omega) \hookrightarrow L_t(\Omega)$ *and* $W^{1,\mathcal{H}}(\Omega) \hookrightarrow W^{1,t}(\Omega)$ *are continuous for all* $t \in [1, p]$*;*
- $W^{1,\mathcal{H}}(\Omega) \hookrightarrow L_t(\Omega)$ *is continuous for all* $t \in [1, p^*]$*;*
- $W^{1,\mathcal{H}}(\Omega) \hookrightarrow L_t(\Omega)$ *is compact for all* $t \in [1, p^*)$*;*
- $W^{1,\mathcal{H}}(\Omega) \hookrightarrow L_t(\partial\Omega)$ *is continuous for all* $t \in [1, p^*]$*;*
- $W^{1,\mathcal{H}}(\Omega) \hookrightarrow L_t(\partial\Omega)$ *is compact for all* $t \in [1, p^*)$*;*
- $L_{\mathcal{H}}(\Omega) \hookrightarrow L^{\mu}_q(\Omega)$ *is continuous.*

2.1. Existence results for double phase problem

Several theoretical works have explored various aspects of our problem, establishing the existence of solutions through different analytical approaches. In particular, numerous studies have investigated problem (P_λ) under specific assumptions on the right-hand side function f. In this framework, we recall the contribution of Lê [6], who, using the Ljusternik–Schnirelmann principle, proved the existence of a solution to problem (P_λ) in the case $f = |u|^{p-2}u$, $\mu = 0$, and $g = 0$. Here, we focus on the case where the parameters involved in problem (P_λ) satisfy the following conditions:

(A_1) $\Omega \subset \mathbb{R}^N$ is a bounded domain with Lipschitz boundary.

(A_2) $1 < p < q < N$, $1 < r \leq p_* = \dfrac{p(N-1)}{N-p}$.

(A_3) $\mu(x) \in L^\infty(\Omega)$, $\mu(x) \geq 0$.

(A_4) $\beta(x) \in L^\infty(\partial\Omega)$, $\beta(x) \geq 0$.

(A_5) The right-hand side $f : \Omega \times \mathbb{R} \to \mathbb{R}$ is a Carathéodory function.

(A_6) There exist constants $C > 0$ and $m \in (1, p^*)$ such that

$$|f(x,u)| \leq C\big(1 + |u|^{m-1}\big), \qquad \forall (x,u) \in \Omega \times \mathbb{R}.$$

(A_7) $g \in L^{r'}(\partial\Omega)$, where r' is the conjugate exponent of r.

Relying on these assumptions, we will next demonstrate that the problem admits a weak solution.

3. Spectrum Analysis

Definition 1 *We say that $\lambda \in \mathbb{R} \setminus \{0\}$ is an eigenvalue of (P_λ) if there exists $u \in W^{1,\mathcal{H}}(\Omega) \setminus \{0\}$ such that for all $v \in W^{1,\mathcal{H}}(\Omega)$, we have:*

$$\int_\Omega \left(|\nabla u|^{p-2}\nabla u + \mu(x)|\nabla u|^{q-2}\nabla u\right) \cdot \nabla v \, dx + \int_{\partial\Omega} \beta(x)|u|^{r-2}uv \, ds = \lambda \int_\Omega f(x,u)v \, dx + \int_{\partial\Omega} gv \, ds. \quad (3.1)$$

Remark 1 *We note that if λ is an eigenvalue of problem (P_λ), then the corresponding eigenfunction $u \in W^{1,\mathcal{H}}(\Omega) \setminus \{0\}$ is a weak solution of problem (P_λ).*

It is well-known that that solving problem (P_λ) is equivalent to finding the optimal pair (u, λ) $W^{1,\mathcal{H}} \times \mathbb{R}^+$ for the following minimization problem:

$$\min_{u \in W^{1,\mathcal{H}}(\Omega),\, u \neq 0} J(u)$$

where

$$J(u) = \int_\Omega \left(\frac{1}{p}|\nabla u|^p + \frac{1}{q}\mu(x)|\nabla u|^q\right) dx + \int_{\partial\Omega} \frac{1}{r}\beta|u|^p \, ds - \lambda \int_\Omega F(x,u) \, dx - \int_{\partial\Omega} gu \, ds$$

represents the variational function associated to the problem (P_λ). We have the next result:

Theorem 1 *Suppose that assumptions A1–A7 are satisfied. Then the functional J attains its minimum at some point $\tilde{u} \in W^{1,\mathcal{H}}(\Omega)$; that is, problem (P_λ) admits a weak solution.*

The proof is established based on the results of the following lemmas:

Lemma 2 *The functional J is well-defined and continuously differentiable.*

Proof: Let $u \in W^{1,\mathcal{H}}(\Omega)$. We need to verify that each of the four terms of $J(u)$ is finite.

- $\int_\Omega \frac{1}{p}|\nabla u|^p \, dx$ and $\int_\Omega \frac{1}{q}\mu(x)|\nabla u|^q \, dx$ are finite by the definition of $W^{1,\mathcal{H}}(\Omega)$ (the modular $\mathcal{H}$ exactly controls these quantities) and because $\mu \in L^\infty(\Omega)$.
- The trace $u|_{\partial\Omega}$ belongs (continuously) to $L^p(\partial\Omega)$ since $W^{1,\mathcal{H}}(\Omega) \hookrightarrow W^{1,p}(\Omega)$ and the trace operator $W^{1,p}(\Omega) \to L^p(\partial\Omega)$ is continuous. As $\beta \in L^\infty(\partial\Omega)$, the product $\beta|u|^p$ is integrable on $\partial\Omega$.
- According to assumption (A_6), there exists $C > 0$ such that

  $$|f(x,t)| \leq C(1 + |t|^{m-1})$$

  with $m \in (1, p^*)$. It follows (by integration with respect to t) that

  $$|F(x,t)| \leq C'(1 + |t|^m).$$

  Since $W^{1,\mathcal{H}}(\Omega) \hookrightarrow L^m(\Omega)$ (continuous Sobolev embedding, as $m < p^*$), we have $u \in L^m(\Omega)$, hence $F(\cdot, u) \in L^1(\Omega)$. Therefore, $\int_\Omega F(x,u) \, dx$ is finite.
- The trace $u|_{\partial\Omega} \in L^r(\partial\Omega)$ (by the assumption $r \leq p_*$) and $g \in L^{r'}(\partial\Omega)$. Hence, by Hölder's inequality, the integral is finite.

  We conclude that $J(u) \in \mathbb{R}$ for all $u \in W^{1,\mathcal{H}}(\Omega)$; therefore, J is well defined.

Proceeding in the same way, one can show that J is of class C^1 on $W^{1,\mathcal{H}}(\Omega)$, since each of its terms is also of class C^1. Then, its derivative is given by:

$$\langle J'(u),v\rangle = \int_\Omega \big(|\nabla u|^{p-2}\nabla u + \mu(x)|\nabla u|^{q-2}\nabla u\big)\cdot\nabla v\,dx + \int_{\partial\Omega}\beta(x)|u|^{p-2}u\,v\,ds$$
$$-\lambda\int_\Omega f(x,u)\,v\,dx - \int_{\partial\Omega} g\,v\,ds.$$

□

Lemma 3 *The functional J is coercive.*

Proof: We need to show that $J(u)\to+\infty$ as $\|u\|_{W^{1,\mathcal{H}}}\to\infty$. It is clear that the main part, formed by the positive terms of J, grows like a power p or q of $\|u\|_{W^{1,\mathcal{H}}}$.
From another perspective, from (A_6), we have: $|f(x,t)|\le C(1+|t|^{m-1})$
Therefore

$$\left|\lambda\int_\Omega F(x,u)\,dx\right| \le \lambda C'\int_\Omega (1+|u|^m)\,dx = \lambda C'\Big(|\Omega| + \|u\|_m^m\Big).$$

Now, by the Sobolev embedding:

$$\|u\|_m \le C_S\|u\|_{1,\mathcal{H}},\quad m<p^*.$$

Therefore,

$$\left|\lambda\int_\Omega F(x,u)\,dx\right| \le \lambda C'\Big(|\Omega| + C_S^m\|u\|_{1,\mathcal{H}}^m\Big).$$

We also have by Hölder's inequality,

$$\left|\int_{\partial\Omega} gu\,ds\right| \le \|g\|_{r'(\partial\Omega)}\,\|u\|_{r(\partial\Omega)}.$$

And the trace satisfies

$$\|u\|_{r(\partial\Omega)} \le C_T\|u\|_{1,\mathcal{H}}.$$

Therefore,

$$\left|\int_{\partial\Omega} gu\,ds\right| \le C_g\,\|u\|_{1,\mathcal{H}}.$$

We thus have

$$J(u) \ge \frac{1}{p}\|\nabla u\|_p^p + \frac{1}{q}\int_\Omega \mu|\nabla u|^q\,dx + \frac{1}{r}\int_{\partial\Omega}\beta|u|^p\,ds - \lambda C' C_S^m\|u\|_{1,\mathcal{H}}^m - C_g\|u\|_{1,\mathcal{H}} - \lambda C'|\Omega|.$$

Since $m<q$ and $p<q$, we can use Young's inequality to absorb $\|u\|_{1,\mathcal{H}}^m$ into $\|u\|_{1,\mathcal{H}}^q$:
for any $\varepsilon>0$, there exists $C_\varepsilon>0$ such that

$$\|u\|_{1,\mathcal{H}}^m \le \varepsilon\|u\|_{1,\mathcal{H}}^q + C_\varepsilon.$$

Then, we choose ε small enough so that $\varepsilon\|u\|_{1,\mathcal{H}}^q$ can be absorbed by $\frac{1}{q}\int_\Omega \mu|\nabla u|^q\,dx$.
The term $C_g\|u\|_{1,\mathcal{H}}$ is negligible compared to the polynomial growth $\|u\|^p$ or $\|u\|^q$ as $\|u\|\to\infty$.

Hence, $J(u)\to+\infty$ as $\|u\|_{1,\mathcal{H}}\to\infty$, proving that J is coercive.

As a result, we obtain a lower bound of polynomial type dominated by q:

$$J(u) \ge A\|u\|_{1,\mathcal{H}}^q - B,$$

for some constants $A, B > 0$ independent of u. Therefore,

$$\lim_{\|u\|_{1,\mathcal{H}} \to \infty} J(u) = +\infty.$$

This is exactly the definition of coercivity. This property ensures that any minimizing sequence of J is bounded in $W^{1,\mathcal{H}}(\Omega)$.

□

Lemma 4 *The functional J is weak lower semi-continuous.*

Proof: We need to prove that for every sequence (u_n) weakly converging $u_n \rightharpoonup u$ in $W^{1,\mathcal{H}}(\Omega)$, we have

$$\liminf_{n\to\infty} J(u_n) \geq J(u).$$

Let us define the positive part of J by:

$$I(u) := \int_\Omega \left(\frac{1}{p} |\nabla u|^p + \frac{1}{q} \mu(x) |\nabla u|^q \right) dx + \int_{\partial\Omega} \frac{1}{r} \beta(x) |u|^p \, ds.$$

The functions $t \mapsto \dfrac{|t|^p}{p}$ and $t \mapsto \dfrac{\mu(x)|t|^q}{q}$ are convex in ∇u, and $t \mapsto \dfrac{\beta |t|^p}{p}$ is convex in $u|_{\partial\Omega}$. Moreover, the integral of convex functions over Ω or $\partial\Omega$ is weakly lower semicontinuous in the reflexive space $W^{1,\mathcal{H}}(\Omega)$. Thus,

$$u_n \rightharpoonup u \quad \Longrightarrow \quad \liminf_{n\to\infty} I(u_n) \geq I(u).$$

On the other hand, we have

$$|F(x, u)| \leq C\big(1 + |u|^m\big), \quad m \in (1, p^*).$$

The weak convergence $u_n \rightharpoonup u$ in $W^{1,\mathcal{H}}(\Omega)$ implies, by the Sobolev compactness embedding,

$$u_n \to u \quad \text{strongly in } L^s(\Omega), \quad 1 \leq s < p^*.$$

Since $m < p^*$, we can choose $s = m$. Hence,

$$u_n \to u \text{ in } L^m(\Omega) \quad \Longrightarrow \quad F(x, u_n) \to F(x, u) \text{ in } L^1(\Omega).$$

Consequently,

$$\int_\Omega F(x, u_n) \, dx \longrightarrow \int_\Omega F(x, u) \, dx \quad \Longrightarrow \quad -\lambda \int_\Omega F(x, u_n) \, dx \longrightarrow -\lambda \int_\Omega F(x, u) \, dx.$$

By the continuity of the trace operator $W^{1,\mathcal{H}}(\Omega) \to L^r(\partial\Omega)$ and since $g \in L^{r'}(\partial\Omega)$, we have

$$u_n \rightharpoonup u \quad \Longrightarrow \quad u_n|_{\partial\Omega} \to u|_{\partial\Omega} \text{ strongly in } L^r(\partial\Omega),$$

and therefore,

$$\int_{\partial\Omega} g u_n \, ds \longrightarrow \int_{\partial\Omega} g u \, ds.$$

Hence, for $u_n \rightharpoonup u$,

$$\begin{aligned}
\liminf_{n\to\infty} J(u_n) &= \liminf_{n\to\infty} \Big[I(u_n) - \lambda \int_\Omega F(x, u_n) \, dx - \int_{\partial\Omega} g u_n \, ds \Big] \\
&\geq \underbrace{\liminf_{n\to\infty} I(u_n)}_{\geq I(u)} - \underbrace{\lim_{n\to\infty} \lambda \int_\Omega F(x, u_n) \, dx}_{= \lambda \int_\Omega F(x,u)\, dx} - \underbrace{\lim_{n\to\infty} \int_{\partial\Omega} g u_n \, ds}_{= \int_{\partial\Omega} g u \, ds} \\
&= I(u) - \lambda \int_\Omega F(x, u) \, dx - \int_{\partial\Omega} g u \, ds \\
&= J(u).
\end{aligned}$$

Therefore, J is weakly lower semicontinuous on $W^{1,\mathcal{H}}(\Omega)$. □

Since J is coercive and weakly lower semi-continuous, and $W^{1,,\mathcal{H}}(\Omega)$ is reflexive, the direct method in the calculus of variations ensures the existence of $u^* \in W^{1,,\mathcal{H}}(\Omega)$ such that:

$$J(u^*) = \inf_{u \in W^{1,p}(\Omega)} J(u).$$

4. Numerical Framework and Simulation

4.1. The proposed algorithm

In this section, we introduce the essential components for developing our algorithm based on Physics-Informed Neural Networks (PINNs) technique, which will subsequently be used to approximate the solution of problem (P_λ). Our goal is to approximate the eigenvalue λ and its associated eigenfunction u in different cases.
Physics-Informed Neural Networks (PINNs) are a methodology that employs neural networks to solve problems governed by physical laws, typically expressed as partial differential equations. By directly incorporating these equations into the training process, PINNs provide an efficient and flexible framework for addressing complex problems in science and engineering [11].

To approximate the minimizer of the functional $J(u)$, we introduce a neural network $u_\theta : \Omega \to \mathbb{R}$, where θ represents the set of trainable parameters including weights and biases.The total loss function is constructed to mirror the functional $J(u)$ and is defined as: $L(\theta) = J(u_\theta)$.
More specifically, we have:

$$\begin{aligned}\mathcal{L}(\theta) = &\int_\Omega \left(\frac{1}{p} |\nabla u_\theta(x)|^p + \mu(x) \frac{1}{q} |\nabla u_\theta(x)|^q \right) dx \\ &+ \frac{1}{r} \int_{\partial\Omega} \beta(x) |u_\theta(x)|^r \, ds - \lambda \int_\Omega F(x, u_\theta(x)) \, dx - \int_{\partial\Omega} g(x) u_\theta(x) \, ds.\end{aligned}$$

These integrals are approximated using a set of collocation points $\{x_i\}_{i=1}^{N_\Omega} \subset \Omega$ and $\{x_j^\partial\}_{j=1}^{N_\partial} \subset \partial\Omega$, which can be sampled uniformly. In practice, these sets may be selected from a fixed mesh or randomly resampled at each iteration of the gradient descent algorithm [11].

To obtain the convergence of the PINNs algorithm, we will focus on the following important theorem:

Theorem 5 *Let $\Omega \subset \mathbb{R}^N$ be a bounded domain with Lipschitz boundary, and let $p > 1$. Consider the functional*

$$J(u) = \int_\Omega \left(\frac{1}{p} |\nabla u|^p + \frac{1}{q} \mu(x) |\nabla u|^q \right) dx + \int_{\partial\Omega} \frac{1}{r} \beta |u|^r \, ds - \lambda \int_\Omega F(x,u) \, dx - \int_{\partial\Omega} g u \, ds$$

where $\beta > 0$, $g \in L^{r'}(\partial\Omega)$.

Assume that $u^\star \in W^{1,\mathcal{H}}(\Omega)$ is a minimizer of J, and that the class of neural networks $\{u_\theta\} \subset C^1(\overline{\Omega})$ is dense in $W^{1,\mathcal{H}}(\Omega) \cap C^1(\overline{\Omega})$ with respect to the $W^{1,\mathcal{H}}$-norm.

If the PINN's is trained so that the residual of the Euler-Lagrange equation and the boundary losses tend to zero as $\theta \to \theta^\star$, then

$$u_\theta \to u^\star \quad \text{in } W^{1,\mathcal{H}}(\Omega), \qquad \text{and} \qquad J[u_\theta] \to J[u^\star].$$

Proof: Since the class of networks $\{u_\theta\}$ is dense in $W^{1,\mathcal{H}}(\Omega) \cap C^1(\overline{\Omega})$, there exists a sequence of networks that can approximate any function in this space arbitrarily well, including the minimizer $u^\star$. The minimizer u satisfies the Euler–Lagrange equation associated with the functional J:

$$\int_\Omega \left(|\nabla u|^{p-2} \nabla u + \mu(x) |\nabla u|^{q-2} \nabla u \right) \cdot \nabla \phi \, dx + \int_{\partial\Omega} \beta(x) |u|^{r-2} u \, \phi \, ds = \lambda \int_\Omega f(x,u) \, \phi \, dx + \int_{\partial\Omega} g \, \phi \, ds,$$

for all $\phi \in W^{1,\mathcal{H}}(\Omega)$.

The functional J is coercive and weakly lower semicontinuous in $W^{1,\mathcal{H}}(\Omega)$ thanks to the convexity of the gradient terms and the boundary terms.

Any minimizing sequence satisfying $J(u_\theta) \to J(u^\star)$ and $J'(u_\theta) \to 0$ converges strongly in $W^{1,\mathcal{H}}(\Omega)$ to the unique minimizer $u^\star$, thanks to the reflexivity of $W^{1,\mathcal{H}}(\Omega)$ and the coercivity of J. Thus, the solution approximated by the PINNs converges strongly in the $W^{1,\mathcal{H}}(\Omega)$ norm and in energy:

$$u_\theta \to u^* \text{ in } W^{1,\mathcal{H}}(\Omega), \quad \text{and} \quad J[u_\theta] \to J[u^*].$$

□

4.2. Numerical experiments

In this section, we evaluate the theoretical results through carefully chosen examples with different parameter values for our problem (P_λ). For all numerical experiments, the algorithm tolerance is set to TOL $= 10^{-5}$, and results are reported with sufficient decimal precision to capture significant differences.

For each given $p, q, r, \mu, \Omega, \beta$, and f, we provide the exact solution, the corresponding eigenvalue, the boundary data, and the errors between exact and numerical values.

It is worth noting that the chosen examples comply with all the assumptions of the theoretical framework, including those for f, p, q, r, β, and μ.

Example 1 *In this first experiment we assume that the exact solution reads:* $u_{ex}(x, y) = \exp(x)\cos(y)$. *Then we have:*

$$f(x,y) = -\big[\exp((p-1)x) + \mu\frac{q-2}{p-2}\exp((q-1)x)\big]\cos y, \quad \lambda = \frac{p-2}{q-2}, q \neq 2.$$

and the boundary data:

$$g_1(x,y) = [\exp((p-2)x) + \mu\exp((q-2)x)]\,\nabla u \cdot \vec{n} + \beta\,\exp((r-1)x)|cosy|^{r-2}\cos(y).$$

The case where p ***and*** q ***are strictly between*** 1 ***and*** 2.
We begin by considering the unit square $\Omega = (0,1) \times (0,1)$. *We summarize the obtained results in Table 1 and Figure 1.*

Table 1: Obtained numerical results for Example 1 on unit square when $1 < p < q < 2$.

p	q	μ	β	λ_{ex}	λ_{app}	error u	error λ	Epoch
1.20	1.40	2.00	3.00	1.333	1.325	1.41×10^{-1}	6×10^{-3}	9000
1.50	1.60	3.00	2.00	1.250	1.231	1.95×10^{-1}	1.9×10^{-3}	12000
1.70	1.90	4.00	7.00	3.000	3.006	7.94×10^{-2}	1.6×10^{-3}	14000

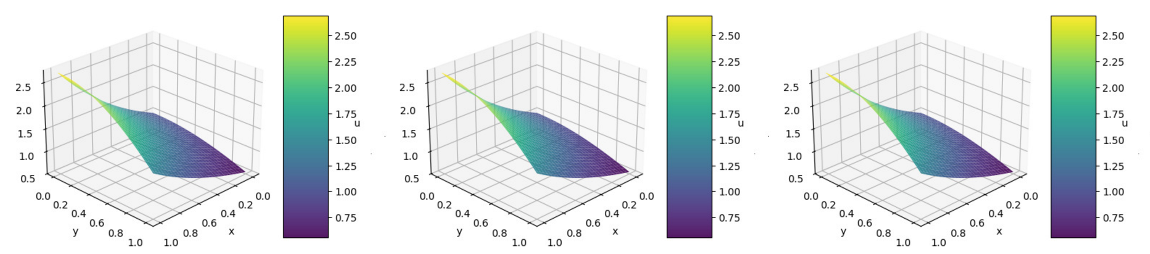

Figure 1: Solution comparison for Example 1 when $p = 1.5$, and $p = 1.7$, with the exact solution at the right, on unit square.

Table 2: Obtained numerical results for Example 1 on unit circle $C^1_{0,0}$ when $1 < p < q < 2$.

p	q	μ	β	λ_{ex}	λ_{app}	error u	error λ	Epoch
1.20	1.40	2.00	3.00	1.333	1.291	2.63×10^{-2}	4.2×10^{-2}	12000
1.50	1.60	3.00	2.00	1.250	1.283	3.1×10^{-2}	3.3×10^{-2}	10000
1.70	1.90	4.00	7.00	3.000	3.012	9.2×10^{-1}	1.29×10^{-2}	14000

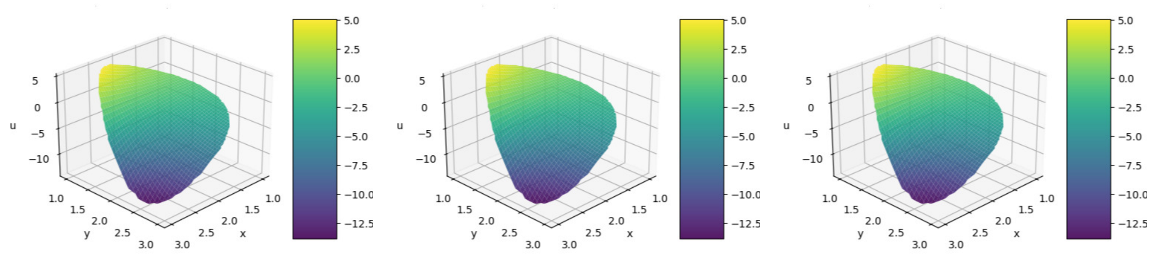

Figure 2: Solution comparison for Example 1 when $p = 1.5$, and $p = 1.7$, with the exact solution at the right, on unit circle.

We now consider the previous example in the unit circle $C^1_{(0,0)}$, and summarize the results in Table 2 and Figure 2.
For each configuration, the previous tables and figures present the parameters defining the double-phase problem, together with the corresponding exact and approximated eigenvalues. They also report the numerical errors associated with both the eigenfunction and the eigenvalue, as well as the number of training epochs required for convergence. The approximated eigenvalues λ_{app} show excellent agreement with the exact ones λ_{ex}, exhibiting relative errors of the order of 10^{-3}. The error on the eigenfunction remains moderate, increasing slightly for larger values of p and q, which also require a higher number of epochs due to the increased nonlinearity of the problem. Overall, these results confirm the accuracy and robustness of the proposed numerical method within the range $1 < p < q < 2$.

Case where p and q are greater than 2.
The comparison of approximated solutions is presented in Figure 3, and the corresponding results obtained in the unit square for $2 < p < q$ are summarized in the Table 3.

Table 3: Obtained numerical results for Example 1 on the unit square when $2 < p < q$.

p	q	p_*	r	μ	β	λ_{ex}	λ_{app}	error u	error λ	Epoch
2.10	4.00	2.39	1.10	3.00	4.00	0.050	0.042	3.12×10^{-2}	8×10^{-3}	9000
3.00	2.10	3.857	3.00	2.00	3.50	10.00	9.981	3.73×10^{-2}	9×10^{-3}	12000
8.00	9.00	36	30.00	20.00	10.00	0.857	0.795	4.35×10^{-2}	6.2×10^{-2}	14000

For the unit circle, we summarize in Table 4, the obtained errors, and in Figure 4 the comparison between exact and approximated eigenfunction.

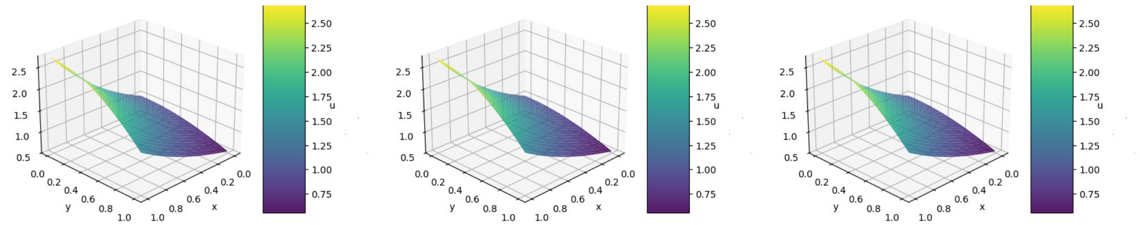

Figure 3: Solution comparison for Example 1 when $(p, q) = (2.1, 4)$ and $(8, 9)$, with the exact solution at the right, on the unit square.

Table 4: Obtained numerical results for Example 1 on the in the circle $C^1_{(0,1)}$ when $2 < p < q$.

p	q	p_*	r	μ	β	λ_{ex}	λ_{app}	error u	error λ	Epoch
2.10	4.00	2.39	1.10	3.00	4.00	0.050	0.043	3.33×10^{-2}	1.7×10^{-2}	11000
3.00	2.10	3.857	3.00	2.00	3.50	10.00	9.973	3.75×10^{-2}	2.7×10^{-2}	9000
8.00	9.00	36	30.00	20.00	10.00	0.857	0.832	3.35×10^{-2}	2.5×10^{-2}	12000

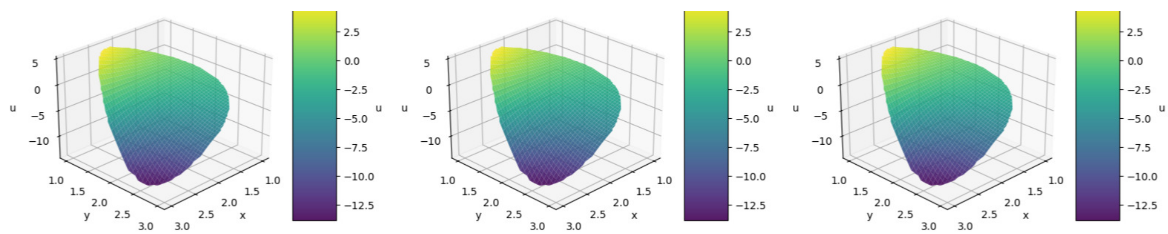

Figure 4: Solution comparison for Example 1 when $(p, q) = (2.1, 4)$ and $(8, 9)$, with the exact solution at the right, on unit circle.

The previous figures demonstrate a strong agreement between the approximated and exact solutions, confirming the validity of our method for the examples considered. From the tables, we observe that the errors on both u and λ are minimal. The number of epochs required to approximate u and λ increases significantly when p and q are larger, which may indicate a higher complexity in the solution process for greater values of p and q.

Example 2 *Let us assume now that $u_{ex}(x, y) = 0.5 \times (x^2 + y^2)$. The other quantities are computed using this exact expression and the expected eigenvalue is given by $\lambda = p/q$.*

Case where p and q are strictly between 1 and 2.
First, we start on the unit square, the obtained results are illustrated in Figure 5 and errors records are summarized in Table 5.

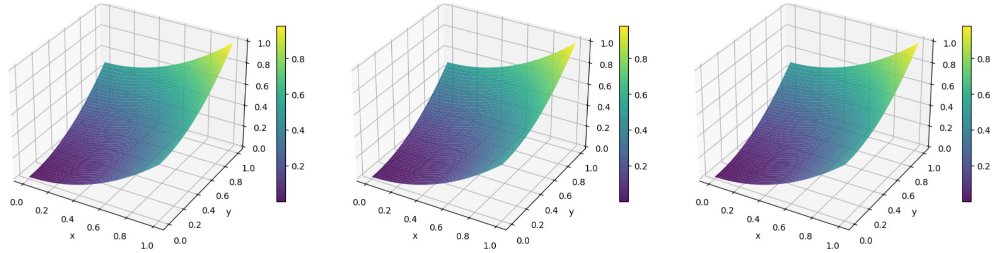

Figure 5: Solution comparison for Example 2 when $p = 1.5$, and $p = 1.8$, with the exact solution at the right, on the unit square.

Table 5: Obtained numerical results for Example 2 on the unit square for $1 < p < q < 2$.

p	q	p_*	r	μ	β	λ_{ex}	λ_{app}	error u	error λ	Epoch
1.20	1.60	1.50	1.40	2.00	3.00	0.750	0.0778	2.31×10^{-2}	2.8×10^{-2}	9000
1.50	1.70	5.00	4.00	5.00	2.00	0.876	0.852	4.77×10^{-2}	2.4×10^{-2}	11000
1.80	1.90	18.00	16.00	3.00	5.00	0.947	0.968	2.25×10^{-2}	2.1×10^{-2}	11000

We now consider the previous example on the unit circle, the comparison of obtained eigenfunctions versus the exact one is illustrated in Figure 6 and errors records in Table 6.

Table 6: Obtained numerical results for Example 2 on the in the circle $C^1_{(0,1)}$ for $1 < p < q < 2$.

p	q	p_*	r	μ	β	λ_{ex}	λ_{app}	error u	error λ	Epoch
1.20	1.60	1.50	1.40	2.00	3.00	0.750	0.732	1.51×10^{-2}	1.8×10^{-2}	9000
1.50	1.70	5.00	4.00	5.00	2.00	0.876	0.854	3.47×10^{-2}	2.2×10^{-2}	12000
1.80	1.90	18.00	16.00	3.00	5.00	0.947	0.956	1.12×10^{-2}	9×10^{-3}	14000

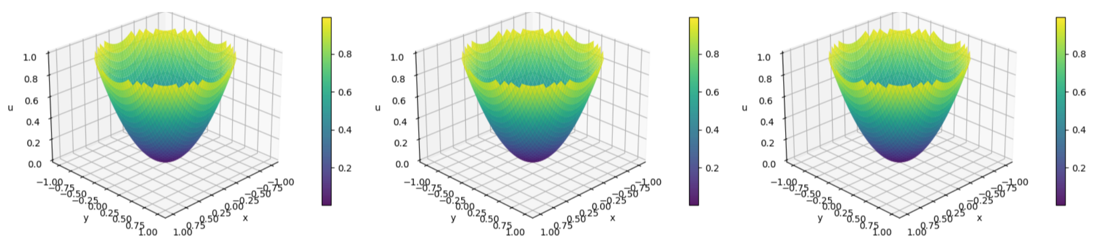

Figure 6: Solution comparison for Example 2 when $p = 2.1$ and $p = 8$, with the exact solution at the right, on the circle.

From previous tables and figures, we can observe that the errors on both the eigenfunction u and the eigenvalue λ remain small across all tested parameter sets, confirming the reliability of the approximation method. Moreover, the number of epochs required for convergence tends to increase as p and q become larger, which suggests that higher parameter values lead to a more complex solution landscape. In addition, the approximated eigenvalues λ_{app} show very good agreement with the exact values λ_{ex}, with relative errors generally below 5%.

Case where p and q greater than 2:
We run our tests for different values of p and q, and we summarize the results in Table 7, Figure 7 on unit square and in Table 8, Figure 8 on unit circle.

Table 7: Obtained numerical results for Example 2 on the unit square when $2 < p < q$.

p	q	p_*	r	μ	β	λ_{ex}	λ_{app}	error u	error λ	Epoch
2.20	2.00	2.53	2.00	3.00	5.00	1.000	1.007	1.47×10^{-2}	9.3×10^{-2}	9000
3.00	7.00	3.85	3.00	2.00	4.00	0.428	0.413	1.67×10^{-2}	1.5×10^{-2}	11000
6.00	9.00	13.50	9.00	5.00	9.00	0.666	0.671	5.23×10^{-2}	5×10^{-3}	12000

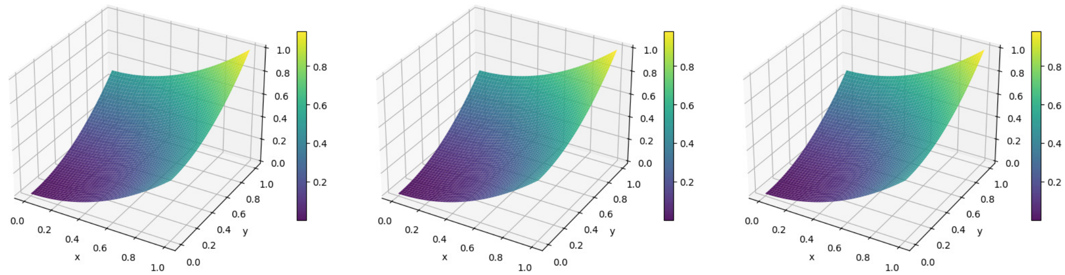

Figure 7: Solution comparison for Example 2 when $p = 2.2$, $p = 3$, and $p = 6$, with the exact solution shown on the right, in the unit square.

Table 8: Obtained numerical results for Example 2 in the circle $C^1_{(0,1)}$ for $2 < p < q$.

p	q	p_*	r	μ	β	λ_{ex}	λ_{app}	error u	error λ	Epoch
2.20	2.00	2.53	2.00	3.00	5.00	1.000	1.013	2.37×10^{-2}	1.3×10^{-2}	9000
3.00	7.00	3.85	3.00	2.00	4.00	0.428	0.406	2.54×10^{-2}	2.2×10^{-2}	11000
6.00	9.00	13.50	9.00	5.00	9.00	0.666	0.658	3.53×10^{-2}	8×10^{-3}	12000

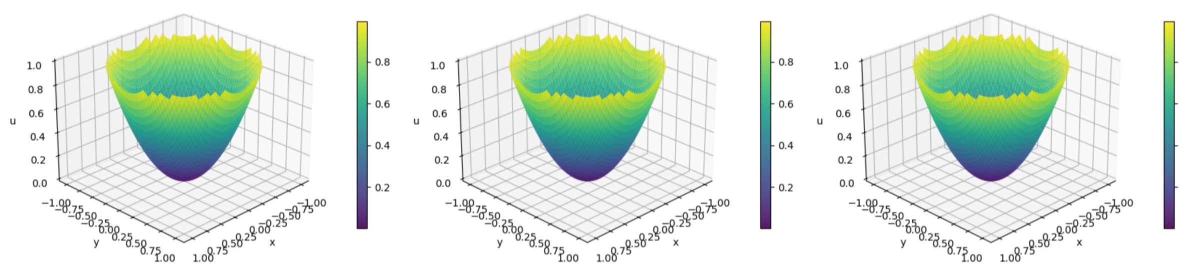

Figure 8: Solution comparison for Example 2 when $p = 2.2$, $p = 3$, and $p = 6$, with the exact solution shown on the right, in the circle $C^1_{(0,1)}$.

Again, the above results confirms the validity of proposed numerical method. Overall, these observations indicate that the proposed method is both robust and accurate across a wide range of parameter values for the considered double-phase problems.

5. Conclusion and Perspectives

In this work, we have studied the Robin double-phase eigenvalue problem. Under appropriate assumptions imposed on the right-hand side function f and on the other parameters, we have guaranteed the existence of a weak solution. The successful implementation of the Physics-Informed Neural Networks method, together with the strong agreement between the numerical and analytical results, highlights the effectiveness of modern computational approaches for solving highly nonlinear differential equations. Future research directions include extending the present study to higher-dimensional settings, exploring alternative boundary conditions, and analyzing more general forms of the double-phase operator to further advance the understanding and applicability of such problems.

References

1. Blanco, C. Á., Gasiński, L., Winkert, P., *A new class of double phase variable exponent problems: Existence and uniqueness*, Journal of Differential Equations, 323, 182–228, (2022).

2. Colasuonno, F., Squassina, M., *Eigenvalues for double phase variational integrals*, Annali di Matematica Pura ed Applicata, 195, 1917–1959, (2016).

3. El Yazidi, Y., Zeng, S., *A splitting-based method for the numerical identification of a nonlinear convection coefficient in elliptic equations*, Mathematics and Computers in Simulation, 235, 205–218, (2025).

4. El Yazidi, Y., Charkaoui, A., Zeng, S., *Finite element solutions for variable exponents double phase problems*, Numer. Algorithms, 1–29, (2025).

5. Gasinski, P. W., *Existence and uniqueness results for double phase problems with convection term*, Journal of Differential Equations, 268, 2183–4193, (2020).

6. Lê, A., *Eigenvalue problems for the p-Laplacian*, Nonlinear Analysis, 64(5), 1057–1099, (2006).

7. Leoni, G., *A First Course in Sobolev Spaces*, 2nd ed., Graduate Studies in Mathematics, Vol. 181, American Mathematical Society, Providence (RI), (2017).

8. Papageorgiou, N. S., Vetro, C. V., *Solutions for parametric double phase Robin problems*, Asymptotic Analysis, 121, 4311–4334, (2021).

9. Papageorgiou, N. S., Zhang, Y., *On the set of positive solutions for resonant Robin* (p, q)*-equations*, Advances in Nonlinear Analysis, 10, 1132–1153, (2021).

10. Papageorgiou, N. S., Zhang, Y., *Existence and multiplicity of solutions for double-phase Robin problems*, Bulletin of the London Mathematical Society, 52, 546–560, (2020).

11. Raissi, M., Perdikaris, P., Karniadakis, G. E., *Physics-informed neural networks: A deep learning framework for solving forward and inverse problems involving nonlinear partial differential equations*, Journal of Computational Physics, 378, 686–707, (2019).

12. Rudin, W., *Functional Analysis*, 2nd ed., McGraw–Hill, New York, (1991).

Research Laboratory of Numerical Analysis, Nonlinear Analysis, and Applications (LaR2A),

Faculty of Sciences, Abdelmalek Essaadi University, Tetouan,, Morocco.

E-mail address: abdelaziz.elbaraymi@etu.uae.ac.ma, y.elyazidi@uae.ac.ma, bferrahi@uae.ac.ma